Discriminative-Region-Aware Residual Network for Adolescent Brain Structure and Cognitive Development Analysis

Yongsheng Pan[1,2], Mingxia Liu[2(✉)], Li Wang[2], Yong Xia[1(✉)], and Dinggang Shen[2(✉)]

[1] School of Computer Science and Engineering, Northwestern Polytechnical University, Xi'an 710072, China
yxia@nwpu.edu.cn
[2] Department of Radiology and BRIC, University of North Carolina at Chapel Hill, Chapel Hill, NC 27599, USA
{mxliu,dgshen}@med.unc.edu

Abstract. The brains of adolescents undergo profound cognitive development, especially the development of fluid intelligence (FI) that is the ability to reason and think logically (independent of acquired knowledge). Such development may be influenced by many factors, such as changes in the brain structure caused by neurodevelopment. Unfortunately, the association between brain structure and fluid intelligence is not well understood. Cross-sectional structural MRI data released by the Adolescent Brain Cognitive Development (ABCD) study pave a way to investigate adolescents' brain structure via MRIs, but each 3D volume may contain irrelevant or even noisy information, thus degrading the learning performance of computer-aided analysis systems. To this end, we propose a discriminative-region-aware residual network (DRNet) to jointly predict FI scores and identify discriminative regions in brain MRIs. Specifically, we first develop a *feature extraction module* (containing several convolutional layers and ResNet blocks) to learn MRI features in a data-driven manner. Based on the learned feature maps, we then propose a *discriminative region identification module* to explicitly determine the weights of different regions in the brain, followed by a *regression module* to predict FI scores. Experimental results on 4,154 subjects with T1-weighted MRIs from ABCD suggest that our method can *not only* predict fluid intelligence scores based on structural MRIs *but also* explicitly specify those discriminative regions in the brain.

1 Introduction

The brains of adolescents undergo profound cognitive development, especially the development of fluid intelligence. Independent of acquired knowledge, fluid intelligence or fluid reasoning is the ability to reason and think logically [1,2],

D. Zhang et al. (Eds.): GLMI 2019, LNCS 11849, pp. 138–146, 2019.
https://doi.org/10.1007/978-3-030-35817-4_17

such as analyzing and solving novel problems, identifying patterns and relationships that underpin these problems and the extrapolation of these using logic. Recent studies are finding that aerobic conditioning, hand-eye coordination, motor skills, and daily physicality are important for maintaining fluid intelligence. With the neurodevelopment in adolescent brains, the resulting changes in brain structure may also influence the development of fluid intelligence. Previous studies have shown that changes in the brain structure can lead to changes in behavior and thinking [3,4]. As an example, many neuroscience studies on children and young adults with autism spectrum disorder demonstrate abnormalities in several brain regions (*e.g.*, hippocampus and precentral gyrus), while studies on old adults with Alzheimer's disease find structural changes in different brain regions (such as hippocampus and amygdala) [5,6]. Unfortunately, the association between adolescent brain structure and fluid intelligence has not been well understood currently. Therefore, bridging this gap is very meaningful for analyzing adolescent brain cognitive development.

Magnetic resonance (MR) examination allows clinicians and researchers to examine brain anatomy in a non-invasive manner. Especially, structural MR imaging (MRI) has been widely used to investigate brain morphology because of its high spatial resolution and contrast sensitivity [7]. Recently, the Adolescent Brain Cognitive Development (ABCD) study [8] released cross-sectional structural MRI data, paving a way to investigate the anatomical structure of adolescent brains via MRIs. Since each 3D volume contains a large number of regions, directly using the whole MR image may degrade the learning performance of computer-aided analysis systems due to those irrelevant or noisy regions.

To address this issue, various MRI-based machine/deep learning methods have been developed, by relying on prior anatomical knowledge or learn discriminative brain regions in a data-driven manner. For example, Zhang *et al.* [9] first defined multiple anatomical landmarks in brain MR images via group comparison, and then extracted image patches based on these landmarks for automated brain disease diagnosis. Li *et al.* [10] developed a multi-channel convolutional neural network (CNN) for identifying autism spectrum disorder, by first detecting anatomical landmarks and then training a CNN model for classification. However, these two methods employed handcrafted MRI features that may not well coordinated the subsequent classifier and treated landmark definition and classifier training as two standalone steps, thus leading to sub-optimal performance. Lian *et al.* [6] proposed a hierarchical fully convolutional network to automatically identify discriminative local patches and regions in the whole brain MRI, upon which task-driven MRI features were then jointly learned and fused to construct hierarchical classification models for disease identification, achieving state-of-the-art performance. However, this method cannot explicitly uncover the importance of different brain regions. Most importantly, existing methods generally focus on adult brains [6,9] or infant brains [10], and hence cannot be directly applied to adolescent brains due to differences in data distribution.

In this paper, we propose a discriminative-region-aware residual network (DRNet) to jointly predict fluid intelligence (FI) scores and identify

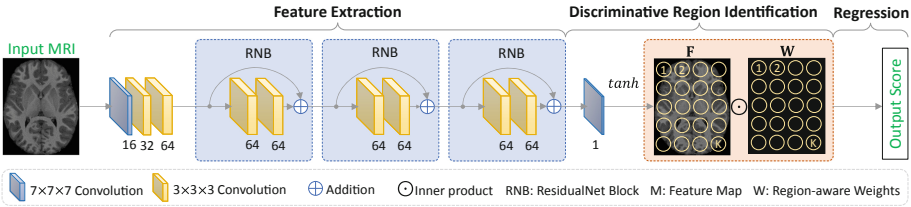

Fig. 1. Illustration of the proposed discriminative-region-aware residual network (DRNet) for joint fluid intelligence (FI) prediction and discriminative brain region identification. Three major components are included in DRNet: (1) a *feature extraction module* with 3 convolutional layers and 3 ResNet blocks (RNB) to learn MRI features, (2) a *discriminative region identification module* to explicitly learn the weights of different brain regions in each MRI, and (3) a *regression module* to estimate the FI score of the input MRI. The learned FI map (*e.g.*, $\mathbf{F}$ containing K regions) are further weighted by the to-be-learned *region-aware weight map* $\mathbf{W}$ (with the same size as $\mathbf{F}$) to automatically discover those discriminative regions for FI score prediction.

discriminative regions in brain MRIs. As shown in Fig. 1, given an input MR image, we first resort to a *feature extraction module* (containing several convolutional layers and ResNet blocks) to learn its features automatically. Based on the learned feature maps, we then design a *discriminative region identification module* to explicitly learn the weights of different regions in each brain MRI, followed by a *regression module* to predict FI scores. To the best of our knowledge, this is almost the first attempts to investigate the association of adolescent brain structure and fluid intelligence using structure MRIs and deep residual networks. Experimental results on 4,154 subjects from ABCD suggest that our method achieves promising results, in comparison to several state-of-the-art methods.

2 Method

Feature Extraction Module: As shown in Fig. 1, the proposed feature extraction contains a backbone with three convolutional layers (with 16, 32, and 64 channels, respectively) and three ResNet Blocks (RNBs) to extract MRI features, as well as a fully-connected layer (with 1 channel) to predict an FI map for all brain regions. In each RNB, there are two subsequent convolutional layers (with 32 channels) and an addition operation. Relu is used as the activation function for all convolutional layers, while *tanh* is used for the fully-connected layer. The strides are set to 2 for the second and third convolutional layers, and 1 for all the other layers. Since the resolution of all images is $1 \times 1 \times 1\text{mm}^3$, the resolution of the output FI maps is $4 \times 4 \times 4$. Given an MR image with the size of $144 \times 176 \times 144$, the output N-channel FI map (denoted as $\mathbf{F} = \{f_1, f_2, \cdots, f_N\}$) is sized of $36 \times 44 \times 36$ (*i.e.*, $K = 51840$ in Fig. 1), with each element corresponding to a specific region around a center location in the original brain MRI.

Discriminative Region Identification Module: It's worth noting that not all of those K regions in the FI maps are related to the task of FI prediction. To select the most discriminative regions, we employ a *region-aware weight map* (denoted as $\mathbf{W} = \{w_1, w_2, \cdots, w_N\}$) to encourage that the output FI maps (*i.e.*, $\mathbf{F}$) should focus on those discriminative regions. The sum of the element-wise product of $\mathbf{W}$ and $\mathbf{F}$ is considered as the final FI score S_{FI} of the input MR image, which could be represented as

$$S_{FI} = \mathbf{W} \odot \mathbf{F} = \Sigma_{n=1}^{N} w_n f_n; \Sigma_{l=1}^{N} w_n = 1. \quad (1)$$

Using Eq. 1, we encourage that those most discriminative regions will contribute more to the final FI prediction result, while the influence of those uninformative brain regions will be suppressed. Another advantage of the proposed discriminative region identification module is that the weights of different brain regions in MRI can be explicitly captured by the region-aware weight map $\mathbf{W}$, and the learning of $\mathbf{W}$ is seamlessly incorporated into the network training process. Such a region-aware weight learning strategy can be flexibly applied to other neuroimage-based deep networks, thus potentially helping reduce the negative influence of uninformative regions in 3D volumes.

Implementation: The proposed network is implemented in Python with TensorFlow. The Adam solver [11] is used with a batch size of 1 and a learning rate of 2×10^{-3}. In the *training* stage, we first pre-train the network without updating the weight matrix (*e.g.*, $\mathbf{W}$) for brain regions, based on all training subjects. We then train the entire DRNet in an end-to-end manner for joint FI score prediction and region weight learning. In the *testing* stage, the structural MR image of an unseen testing subject is fed into the DRNet, and the predicted FI score will be obtained for this subject.

3 Experiment

3.1 Materials and Image Pre-processing

A cross-section of T1-weighted MR imaging data and the corresponding fluid intelligence scores for children aged 9–10 years were downloaded online (https://nda.nih.gov/edit_collection.html?id=2573). These subjects were partitioned into two subsets, including (1) training set with 3,739 subjects, and (2) validation set with 415 subjects. Fluid intelligence scores of all subjects were measured by the ABCD study using the NIH Toolbox Neurocognition battery [12].

We employed our in-house tools to pre-process all T1-weighted MR images. A standard pipeline for image pre-processing include the following eight procedures, including (1) anterior commissure (AC)-posterior commissure (PC) alignment; (2) skull stripping; (3) intensity correction; (4) cerebellum removal; (5) linear alignment to the Colin27 template; (6) re-sampling all images to have the same size of $181 \times 217 \times 181\,\mathrm{mm}^3$ (with a spatial resolution of $1 \times 1 \times 1\,\mathrm{mm}^3$); (7) cropping each image to $144 \times 176 \times 144\,\mathrm{mm}^3$ to remove the background; and (8) performing intensity inhomogeneity correction by using N3 algorithm.

Table 1. Results of FI score prediction achieved by five different methods on the training data using 5-fold cross-validation.

Method	Fold #1		Fold #2		Fold #3		Fold #4		Fold #5	
	MAE	MSE	MAE	MSE	MAE	MSE	MAE	MSE	MAE	MSE
RVR [13]	7.09	78.32	7.24	83.38	7.35	88.74	7.33	84.90	7.17	85.63
CNN [14]	7.10	79.55	7.22	83.38	7.37	89.28	7.38	85.86	7.19	86.41
DSNN [15]	7.10	77.84	7.26	83.67	7.34	88.64	7.32	84.71	7.18	85.51
DRNet_now	7.09	77.97	7.27	83.80	7.43	90.36	7.33	84.97	7.19	85.54
DRNet (Ours)	7.05	77.37	7.24	83.16	7.33	88.16	7.29	84.37	7.13	85.37

3.2 Experimental Setup

We compared the proposed DRNet with two baseline methods and a state-of-the-art method for MRI-based regression, including (1) region-based volumetric representation (RVR) [13], (2) a conventional convolutional neural network (CNN) [14], and (3) disease-image specific neural network (DSNN) [15]. To evaluate the effect of the proposed discriminative region identification module, we further compare DRNet with its variant that does not contain the region-aware weight map (*i.e.*, $\mathbf{W}$), and call this method as "DRNet_now". For the fair comparison, our DRNet and four competing methods share the same input MRIs and output FI scores. The details of the competing methods are listed as follows.

(1) **RVR** [13]. In this method, each brain MRI is first segmented into three tissue types, *i.e.*, gray matter (GM), white matter (WM) and cerebrospinal fluid (CSF). The AAL template with 90 pre-defined regions-of-interest in cortical and sub-cortical regions was further aligned to each MR image via nonlinear image registration. Finally, normalized volumes of GM tissue inside those 90 ROIs are concatenated to be the feature representation of each MRI, followed by a linear support vector regressor (with default parameters) for FI score regression.

(2) **CNN** [14]. In this method, each input MR image is fed to a sequence of 9 convolutional layers, with the channel numbers of 16, 32, 64, 64, 64, 64, 64, 64, 64, respectively. The generated feature maps are further fed into a fully-connected layer (with 1 channel) to predict the FI score of each subject. Similar to our DRNet, all convolutional layers employ the Relu activation function, while the fully-connected layer use *tanh* as the activation function.

(3) **DSNN** [15]. The DSNN method contains a feature extraction module and a spatial cosine module. There are 5 convolutional layers in the feature extraction module, with 16, 32, 64, 64, and 64 channels, respectively. Among these five layers, the first 4 and the last Conv layers are respectively followed by the max-pooling and average-pooling with the stride of 2 and the size of 3×3. The spatial cosine module in DSNN was used to l_2-normalize the feature vectors in feature map of the 5^{th} convolutional layer and concatenates them to be spatial representation, followed by a fully-connected layer with cosine kernel to estimate the FI score of a subject.

(4) **DRNet_now**. The network architecture of DRNet_now is similar to that of our DRNet. Specifically, each input MRI is fed into the feature extraction module (see Fig. 1), followed by a fully-connected layer (with *tanh* activation function) for predicting the FI score. That is, DRNet_now cannot explicitly learn the region weights from data.

In the experiments, we used two evaluation metrics to measure the quality of predicted FI scores generated by different methods, including (1) the mean absolute error (MAE), and (2) the mean square error (MSE).

3.3 Cross-validation Results on Training Data

In the first group of experiments, we compared the proposed DRNet with four competing methods using a five-fold cross-validation strategy on the training data. Specifically, we randomly partitioned the training data to five folds (with roughly equal size). Each time, one fold was used as the testing set and the remaining folds were combined to be the training set for training a specific regression model.

The MAE and MSE results of the predicted FI scores achieved by five methods are shown in Table 1. From this table, one may have the following observations. *First*, four deep learning methods (*i.e.*, CNN, DSNN, DRNet_now and DRNet) that learn task-specific MRI features usually perform better than RVR that use handcrafted features. *Second*, the overall performance of our DRNet is slightly better than that of the other methods. This implies that explicitly considering the weights of different brain regions (as we do in DRNet) is useful to promote the prediction results for FI scores. *Besides*, our DRNet consistently outperforms its variant DRNet_now among all five folds, suggesting the effectiveness of the proposed region-aware weight learning strategy.

3.4 Results on Validation Data

In the second group of experiments, we first trained five models (*i.e.*, RVR, CNN, DSNN, DRNet_now and DRNet) on all training data and evaluated them on 415 subjects in the validation set. The MAE and MSE results achieved by these five methods are reported in Table 2. Results in Table 2 verify again that our DRNet generally outperforms four competing methods in MRI-based FI score prediction. On the other hand, from Tables 1 and 2, we can see that the overall performance achieved by five methods on the validation data is better than that on the training data (using cross-validation). The possible reason is that the models in Table 2 are trained using all subjects in the training set to produce more powerful predictive models, while those in Table 2 are trained only using 80% training data in each fold. This demonstrates that using more data could further improve the robustness of the trained models.

3.5 Identified Discriminative Regions

We now show the learned region-aware weight map (*i.e.*, $\mathbf{W}$) in Fig. 2. From this figure, one can observe that different brain regions do contribute differently to the

Table 2. Results of FI score prediction achieved by five different methods on validation data (with models learned on the training data).

Method	RVR [13]		CNN [14]		DSNN [15]		DRNet_now		DRNet (Ours)	
	MAE	MSE	MAE	MSE	MAE	MSE	MAE	MSE	MAE	MSE
Result	6.48	71.58	6.81	75.70	6.47	70.81	6.46	70.88	6.45	70.79

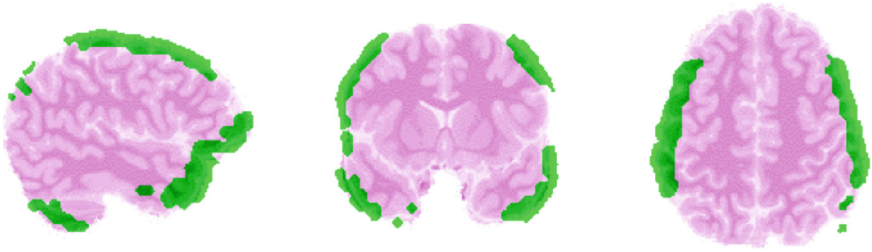

Fig. 2. Region-aware weight map (*i.e.*, **W** in Eq. 1) learned by our proposed DRNet for structural MRIs in ABCD, where the green region is discriminative to FI.

task of FI score prediction. This further validates the rationality of our proposed region-aware weight learning strategy in DRNet. Also, this figure suggests that the most discriminative regions located in the parietal cortex and the frontal cortex, which is consistent with previous studies [16].

3.6 Limitations and Future Work

There are still several limitations to be addressed, listed in the following. *First*, in the current work, we don't consider data distribution differences among different imaging sites, *e.g.*, caused by different populations, while those MRIs in ABCD were acquired from 21 different sites. It is desirable to develop an efficient data harmonization strategy to explicitly alleviate the negative influence of different data distributions in multiple sites. *Second*, we simply employ T1-weighted MR images in the experiments, while subjects in ABCD have multi-modal neuroimages (*e.g.*, T2-weighted MRI and functional MRI). In the future, we plan to take advantage of these multi-modal neuroimaging data to further improve the learning performance, by extending our DRNet to a multi-modal framework. *Besides*, we only consider imaging data in the current network, while demographic information (*e.g.*, age and gender) of subjects may also be associated with brain status. Therefore, it's reasonable to incorporate the demographic information to the model learning process to further improve the prediction results, which will also be our future work.

4 Conclusion

In this paper, we proposed a discriminative-region-aware residual network (DRNet), based on which one can jointly predict FI scores and identify discriminative regions in brain MRIs. Specifically, a feature extraction module was designed to learn MRI features from data automatically. A discriminative region identification module was further designed to explicitly learn the weights of different regions in each brain MRI, followed by a regression module to predict the FI score of the input MR image. Experimental results on 4, 154 subjects from the ABCD study suggest the efficacy of our method in both tasks of fluid intelligence prediction and discriminative brain region identification.

References

1. Carroll, J.B., et al.: Human Cognitive Abilities: A Survey of Factor-analytic Studies. Cambridge University Press, Cambridge (1993)
2. Jaeggi, S.M., Buschkuehl, M., Jonides, J., Perrig, W.J.: Improving fluid intelligence with training on working memory. Proc. Nat. Acad. Sci. U.S.A. **105**(19), 6829–6833 (2008)
3. Casey, B., Giedd, J.N., Thomas, K.M.: Structural and functional brain development and its relation to cognitive development. Biol. Psychol. **54**(1–3), 241–257 (2000)
4. Casey, B., Getz, S., Galvan, A.: The adolescent brain. Dev. Rev. **28**(1), 62–77 (2008)
5. Baron, J., Chetelat, G., Desgranges, B., Perchey, G., Landeau, B., De La Sayette, V., Eustache, F.: In vivo mapping of gray matter loss with voxel-based morphometry in mild Alzheimer's disease. NeuroImage **14**(2), 298–309 (2001)
6. Lian, C., Liu, M., Zhang, J., Shen, D.: Hierarchical fully convolutional network for joint atrophy localization and Alzheimer's disease diagnosis using structural MRI. IEEE Trans. Pattern Anal. Mach. Intell. (2018)
7. Giedd, J.N., et al.: Brain development during childhood and adolescence: a longitudinal MRI study. Nat. Neurosci. **2**(10), 861 (1999)
8. Volkow, N.D., Koob, G.F., Croyle, R.T., Bianchi, D.W., Gordon, J.A., Koroshetz, W.J., Pérez-Stable, E.J., Riley, W.T., Bloch, M.H., Conway, K., et al.: The conception of the ABCD study: from substance use to a broad NIH collaboration. Dev. Cogn. Neurosci. **32**, 4–7 (2018)
9. Zhang, J., Gao, Y., Gao, Y., Munsell, B.C., Shen, D.: Detecting anatomical landmarks for fast Alzheimer's disease diagnosis. IEEE Trans. Med. Imaging **35**(12), 2524–2533 (2016)
10. Li, G., Liu, M., Sun, Q., Shen, D., Wang, L.: Early diagnosis of autism disease by multi-channel CNNs. In: Shi, Y., Suk, H.-I., Liu, M. (eds.) MLMI 2018. LNCS, vol. 11046, pp. 303–309. Springer, Cham (2018). https://doi.org/10.1007/978-3-030-00919-9_35
11. Kingma, D.P., Ba, J.: Adam: a method for stochastic optimization. arXiv preprint arXiv:1412.6980 (2014)
12. Akshoomoff, N., et al.: NIH toolbox cognitive function battery (NIHTB-CFB): measuring executive function and attention. Monogr. Soc. Res. Child. Dev. **78**, 119–132 (2013)

13. Liu, M., Zhang, J., Yap, P.T., Shen, D.: View-aligned hypergraph learning for Alzheimer's disease diagnosis with incomplete multi-modality data. Med. Image Anal. **36**, 123–134 (2017)
14. Krizhevsky, A., Sutskever, I., Hinton, G.E.: Imagenet classification with deep convolutional neural networks. In: NIPS, pp. 1097–1105 (2012)
15. Pan, Y., Liu, M., Lian, C., Xia, Y., Shen, D.: Disease-image specific generative adversarial network for brain disease diagnosis with incomplete multi-modal neuroimages. In: Shen, D., et al. (eds.) MICCAI 2019. LNCS, vol. 11766, pp. 137–145. Springer, Cham (2019)
16. Jung, R.E., Haier, R.J.: The parieto-frontal integration theory (P-FIT) of intelligence: converging neuroimaging evidence. Behav. Brain Sci. **30**(2), 135–154 (2007)